# CHAPTER 100

# WAVE-INDUCED PORE PRESSURE IN RUBBLE MOUND BREAKWATERS

Oumeraci, H.; Partenscky, H.W.

#### Abstract

Experimental results from large scale tests are presented for the distribution of wave-induced pore pressure within rubble mound breakwaters, for the reflection coefficients and the damping of wave motion through the armour and under-layer. The results are then discussed with respect to application and further research.

#### 1. Introduction

Previously, the effects of the internal flow field on the armour and geotechnical stability of rubble mound breakwaters were largely ignored. A brief literature review /3/ as well as recent hydraulic and numerical model investigations /14; 7; 1/ highlighted the importance of the motion of pore water for a better understanding of the geotechnical behaviour and of the external flow on and in the armour layer.

At present, numerical modelling efforts appear to be directed towards the elaboration of an integrated code which should describe wave action on and within the breakwater as well as its effect on armour stability.

Considering the present knowledge of scale effects /8; 13; 4/ and owing to the fact that the loading parameters are not controllable under prototype conditions, measurements from large scale model tests at present represent the most suitable data for calibration and verification. Thus, it is one of the main objectives of this paper to provide the necessary information for this purpose.

<sup>1</sup> Franzius-Institute, University of Hannover, Germany

#### 2. Oscillatory Flow in Porous Media-Theory

When a wave approaches a non-overtopped rubble mound breakwater, part of the incident energy  $\mathrm{E}_i$  is dissipated on and within the structure  $(\mathrm{E}_d)$ , part is reflected  $(\mathrm{E}_r)$  and the rest is transmitted  $(\mathrm{E}_t)$  through the breakwater:

$$E_i = E_d + E_r + E_t \tag{1}$$

The dissipated energy (E $_{d}$ ) can in turn be divided in three distinct parts: the energy dissipated on and in the armour layer (E $_{da}$ ), the energy dissipated in the under layer filter (E $_{df}$ ) and the energy dissipated within the core (E $_{dc}$ ):

$$E_{d} = E_{da} + E_{df} + E_{dc}$$
 (2)

Most of the studies available on waves in rubble mound breakwaters are directed more toward the determination of averaged transmission and reflection coefficients than toward the understanding of the internal wave motion; i.e. the porous structure is often considered as a kind of a black box system.

Theoretical work which actually deals with the internal oscillatory flow induced by waves was mostly related to the study of permeable wave absorbers and wave filters /2; 9; 11/. In this respect, BIESEL /2/ was the first to identify the form of the spatial and temporal relationships which describe a linearly damped, oscillatory flow. LE MEHAUTE /10/ continued BIESEL's work and applied it to rubble mound breakwaters.

The investigations of BIESEL /2/ and LE MEHAUTE /10/ are considered here because a) they constitute the first attempts to describe wave motion in porous media and b) almost no significant advances on their fundamental approach have been made since then.

A general linearized BERNOULLI equation for an oscillatory flow in a wave filter based on the NAVIER-STOKES equation has been derived by BIESEL /2/.

A parameter  $k_V$  = D/n was introduced in this equation by LE MEHAUTE /10/ to account for the porosity n and inertia effects (D) of the porous material:

$$\frac{p}{o} + k_V \frac{\partial \phi}{\partial t} + g y + c_f \phi = const.$$
 (3)

The time derivative of equ. (3), together with  $\frac{\partial y}{\partial t} = \frac{1}{n} \frac{\partial \phi}{\partial y}$  and p = const. at the free surface y = f(x,t) yields:

$$k_{V} \frac{\partial^{2} \phi}{\partial t^{2}} + \frac{g}{n} \frac{\partial \phi}{\partial y} + c_{f} \frac{\partial \phi}{\partial t} = 0$$
 (4)

where:

g = acceleration of gravity

p = pore pressure
ρ = water density

cf = linearized friction coefficient

 $\phi^{-}$  = potential function of a 2D-wave travelling through a porous medium with a porosity n and subject to a friction force  $F_{R}^{-}$  =  $-c_{f} \cdot grad \phi$ 

t = time

x,y = coordinates (Ox-axis is at SWL and Oy-axis is positive upward)

Considering the continuity equation  $\Delta \phi = 0$  and the boundary condition at the depth y = -h, the following particular solution of equ. (4) is obtained.

$$\phi = \frac{H_W}{2} e^{-\beta k x} \frac{\omega}{k \sinh k h} | \cos \beta k (h+y)$$

$$\cosh k (h+y) \sin (kx - \omega t) + \sin \beta k (h+y)$$

$$\sinh k (h+y) \cos (kx - \omega t) | (5)$$

where:

 $H_{\mathbf{W}}$  = incident wave height at the outer boundary of the porous medium (x = 0)

h = water depth

 $k = 2\pi/L'$ : wave number

L' = wave length within the breakwater

ω = 2π/T: angular wave frequency

T = wave period

B = damping coefficient

The wave length L' within the rubble mound breakwater is related to the length L of the incident wave as follows /10/:

$$L' = L/\sqrt{D} \text{ for } h/L < 0.5$$
 (6)

where:

$$L = \frac{gT^2}{2\pi} \tanh \frac{2\pi h}{L}$$
 (7)

D : Coefficient characterising the relative increase of the seapage length as a result of the deviation of the flow path caused by the presence of the grains. An empirical value D  $\approx$  1.4 was given by LE MEHAUTE /10/, whereas a value D = 1.5 was determined theoretically by MICHE /12/.

It follows from equ. (5) and (6) that the height of the pressure oscillation p(x) of a wave travelling through a rubble mound breakwater in the x-direction will decrease exponentially according to the following expression:

$$p(x) = p_0 \cdot e^{-\beta \frac{2\pi}{L^T}} x$$
 (8)

where  $p_0 = pore pressure at x = 0$ 

#### 3. Experimental Set-up and Test Procedure

### 3.1 Description of the breakwater model

The rubble mound breakwater model tested and the experimental set-up have already been described in a previous paper /3/. The cross-section of the large scale model with the position of the pressure cells and the runup gauges is shown in Fig. 1.

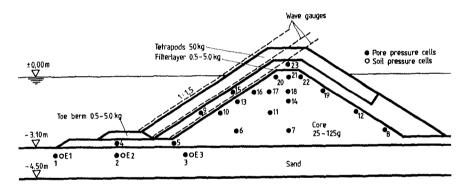


Figure 1. Large scale model of the investigated breakwater

The grain size distribution of the core material used in the model is given in /3/.

The mean diameter is  $d_{50} \approx 4$  cm and the uniformity coefficient U =  $\frac{d_{60}}{d_{10}} \approx 2.2$ . For the wave heights tested the REYNOLDS number related to the grain size is in the range Re =  $5 \cdot 10^4$  to  $10^5$ ; i.e. scale effects due to viscous flow within the core material can be neglected /13/.

#### 3.2 Test programme and procedure

For each test series the wave period was kept constant, whereas the wave height was increased after each test.

Monochromatic waves with heights up to 2.0 m and periods T = 3 - 8 s, as well as irregular waves with significant heights up to 1.0 m and peak periods  $T_p = 3 - 8$  s have been used. In addition, 4 test series with the most critical peak period ( $T_p = 4.5$  s) were carried out for groupiness factors GF = 0.6, 0.7, 0.8 and 0.9 in order to investigate the effect of wave grouping on wave run-up, internal pressure build-up and armour stability.

During the tests, attention has been placed on observations of armour stability as well as on simultaneous measurements of incident waves, pore pressure distribution and wave run-up on the slope of the armour, filter layer and core material.

#### 4. Experimental Results

#### 4.1 Wave reflection

The incident and reflected waves have been determined by means of the commonly used 3-wave gauge procedure. For the range of wave conditions tested, the reflection coefficient  $K_R$  is given in Fig. 2 as a function of the surf similarity parameter  $\xi$ .

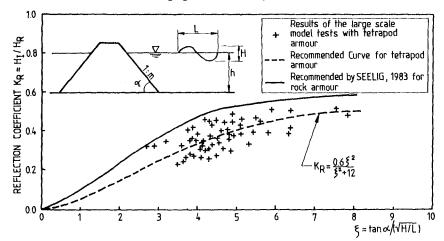


Figure 2. Reflection coefficient  $K_R$  vs. surf similarity parameter  $\xi$ 

The reflection coefficients obtained (K $_{\rm R}=0.20-0.45$ ) correspond to the values given by SOFREMER and SOGREAH for tetrapods, but are comparatively lower than those given by the empirical relationship derived by CERC /14/ for natural stone armours. The latter appears to rather describe the envelope of the maximum values for the tetrapod armour (Fig. 2).

#### 4.2 Wave damping by the armour and under-layer

The incident waves penetrating into the armour and under-layer as well as into the core are followed by means of 3 wave run-up gauges. They have been specially developed for this purpose and were installed along the slope of the tetrapod armour, of the under-layer and of the core material, respectively ((Fig. 1).

The analysis of the results shows that a considerable part of the incident wave energy is dissipated not only by the armour but also by the under-layer. The degree of dissipation is strongly dependent on the magnitude of the similarity parameter  $\xi$ . The smaller this parameter, the more pronounced is the energy dissipation. For instance, the drop of the relative wave height when the wave passes through the armour layer varies from about 30 % to 60 % for surf similarity parameters  $\xi=5$  and  $\xi=2$ , respectively. Considering the total attenuation of wave motion taking place within both the armour and the underlayer, the corresponding values become 60 % to 90 %, respectively (Fig. 3).

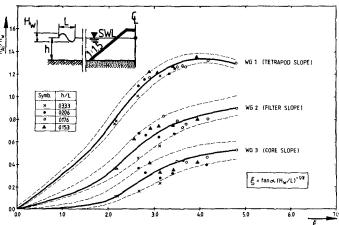


Figure 3. Wave damping by the armour and under-layer vs. surf similarity parameter  $\xi$ 

The dependence of the energy dissipation on the surf similarity parameter  $\xi$  results from the shape of breakers on the outer slope; i.e. spilling and plunging breakers ( $\xi \le 2$ ) which are associated with a high degree of air entrainment and high impact velocities give the largest damping values, whereas collapsing and surging breakers ( $\xi \ge 2$ ) yield the lowest ones.

A further result emerging from Fig. 3 is the much lower value of the run-up and run-down heights on the core slope compared to that at the outer slope. This is of importance for the design of the crest level of the core material. However, a set-up of the mean water level inside the breakwater, which may range from 10 to 20 % of the incident local wave height, should be additionally considered.

#### 5. Wave-Induced Pore Pressure

For the measurement of the pore pressure inside the rubble mound breakwater model twenty piezoresistive pressure gauges (Type PDCR NATEC SCHULTHEISS) were installed at different locations (Fig. 1). These locations were selected in such a way that the pore pressure distribution and the boundary values required for the implementation and calibration of numerical models can be gained with sufficient accuracy.

The designation "pore pressure" used in the following is related to the excess pore water pressure which is solely induced by wave action; i.e. all the twenty pressure gauges record zero pressure at still water level (no wave action). Thus, the corresponding hydrostatic pressure head should be added to the recorded pressure values to obtain the total pore water pressure. The terms "pore pressure height" and "pore pressure amplitude" are used on the analogy with waves to designate the height and the amplitude of the pressure fluctuations, respectively.

5.1 Influence of incident wave parameters on pore pressure

#### 5.1.1 Effect of wave height

The effect of the incident wave height on the magnitude of the pore pressure is illustrated for one location in Fig. 4.

Given a wave period and with increasing wave heights the pore pressures first increase rapidly, then at a lower rate, due to higher friction losses associated with larger hydraulic gradients. The pore pressure - wave height curves appear to have a similar shape for the locations and wave periods investigated.

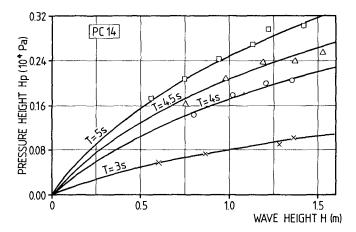


Figure 4. Effect of wave height on pore pressure

# 5.1.2 Effect of wave period

The effect of the incident wave period on the magnitude of the pore pressure is shown in Fig. 5.

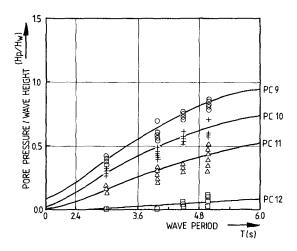


Figure 5. Effect of wave period on pore pressure

Given a wave height and with increasing wave period the pore pressure first increases very slightly, then rapidly and finally at a lower rate.

Similar shapes of pore pressure - wave period curves have been obtained for further locations and various wave heights.

#### 5.2 Spatial distribution of pore pressure

In the following, only the spatial distribution of time averaged values of pore pressure heights is considered. In this respect and for simplification, the horizontal and the vertical distributions are treated separately.

# 5.2.1 Horizontal pore pressure distribution

In order to verify whether the waves are damped within the breakwater according to the theory outlined in chapter 2, the horizontal plane containing the pressure cells PC 15 to PC 19 is considered (Fig. 1). For this purpose, the ratio between pore pressure p(x') at a distance x' from the origin located at PC 15 (x'=0) and pore pressure  $p_0$  measured at x'=0 is plotted against the relative distance x'/L'.

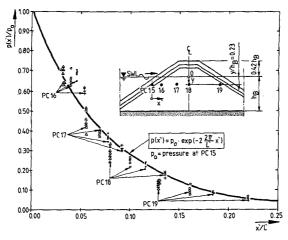


Figure 6. Pore pressure dissipation within the breakwater

For the elevation of the horizontal plane considered, the pore pressure decreases exponentially in the direction of wave propagation according to the following relationship:

$$p(x') = p_O \cdot e^{-2 \cdot \frac{2\pi}{L'} x'}$$
 (9)

However, the magnitude of the damping factor ß in equ. (8) depends on the elevation of the horizontal plane considered with respect to the still water level (SWL). Further results which will be published in the near future suggest that the lower the location under SWL, the smaller the damping factor ß becomes. This can be explained by the friction losses which become smaller as the degree of turbulence decreases, i.e. as the distance from SWL increases.

# 5.2.2 Vertical pore pressure distribution

The pore pressure does not vary hydrostatically with depth, even in the centre of the breakwater. This may be explained by the dynamic effects which are more pronounced near the front face and just under SWL. In order to identify the relevant parameters which influence the degree of attenuation with depth, the relative pore pressure height p(y)/ $H_{\rm W}$  is plotted against the relative elevation (y/L) under SWL in Fig. 7 for different relative water

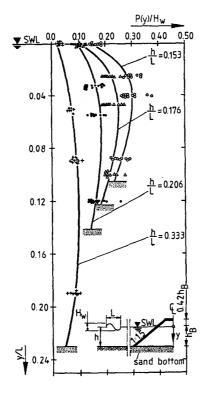


Figure 7. Pore pressure attenuation with depth

depths (h/L). Departing from SWL the pore pressure first increases up to a maximum value with increasing depth, then slightly decreases. The smaller the relative water depth (h/L), i.e. the longer the waves, the higher is the induced pore pressure and the less pronounced is the pressure attenuation.

#### 6. Discussion and Application of the Results

#### 6.1 Reflection coefficient

An accurate evaluation of the reflection coefficient  $K_R = \sqrt{E_r/E_i}$  is important, since it is the remaining energy  $E_{dt} = E_{d} - E_{t}$  (see equ. (1)) which represents the input for the study of energy dissipation on and in the breakwater. Thus rewriting equ. (1) as:

$$E_{dt} = E_{d} + E_{t} = (1 - K_{R}^{2})E_{i},$$
 (10)

it follows from the relationship obtained in Fig. 2 that  $E_{\rm dt}$  may amount to 80 - 96 %, depending on the surf similarity parameter  $\xi.$  For the range of common  $\xi-$ values this relationship can be used for tetrapod armours. It is suggested, however, that future work should focus upon the development of more suitable measuring techniques and methods for the determination of reflection coefficients, since the 3 wave gauge procedure commonly used is still not satisfactory.

#### 6.2 Energy dissipation through armour and under-layer

The results shown in Fig. 3 represent the first attempts to follow the wave motion from the sea-structure interface to the core. For this kind of investigation, small-scale model tests are not suitable because of the dissimilarity of air entrainment resulting from breaking waves and flow separation. For the importance of air content for energy dissipation on and in the breakwater see chapt. 6.4. A reliable evaluation of the rate of energy dissipation through the first layers does not only provide the necessary boundary conditions for resolving the equations of motion in numerical codes, but also helps in assessing the forces on armour units.

Together with the relationship given in Fig. 2, the results presented in Fig. 3 allows the evaluation of the different energy components involved in equ. (1) and (2). For instance, given a surf similarity parameter  $\xi=4$ , the reflected energy is  $E_{\rm r}=12$  %, the energy dissipated on and in the armour layer  $E_{\rm da}=54$  %, the part dissipated in the under-layer  $E_{\rm df}=23$  % and the remaining part which

is finally transmitted into the breakwater core is only ll % of the total incident wave energy.

These results implicitly highlight the importance of the armour and the under-layer for energy dissipation and the question which may arise if a single armour layer is used or an under-layer is omitted.

# 6.3 Attenuation of pore pressure within the breakwater

The experimental results presented here generally give much higher pressure values when compared to the results from available numerical codes /1; 5; 6/. This is mainly due to the fact that the dynamic component of the pore pressure has not been well accounted for. The latter, however, represents an important part of the total wave-induced pore pressure, particularly in the region under SWL and near the front face where it is more dominant.

#### 6.4 Some remarks on scale effects

The limitations of common small scale model tests when investigating wave energy dissipation on and within rubble mound breakwaters are due to the impossibility of simultaneously fulfilling the similitude criteria of FROUDE, WEBER and REYNOLDS.

# a) Scale effects due to the dissimilarity of WEBER's number

The rate of air entrainment into the armour and underlayer resulting essentially from wave breaking, and to a lesser extent from flow separation, is generally higher in prototype; i.e. the rate of wave energy dissipation through the armour and under-layer is lower in the model. The relationship between air entrainment and energy dissipation in breaking waves has already been treated by FÜHRBÖTER /4/. In addition, it has been observed (video records) that a large amount of air bubbles are often driven into the core by breaking waves. The effect of air content  $\alpha$  in the two-phase internal flow, however, is known to cause a reduction of the effective hydraulic conductivity of the porous medium /6; 5/:

$$K_{aW} = K_W (1 - \alpha)^3$$
 (11)

where  $K_{aw}$ ,  $K_w$ : two-phase and single-phase hydraulic conductivity, respectively.

This means that an air fraction  $\alpha$  of only 10 % may cause a reduction of more than 25 % in the hydraulic conductivity. This in turn will considerably reduce the rate of pore pressure attenuation.

b) Scale effects due to the dissimilarity of REYNOLDS' number

The use of small-scale models generally results in a lower permeability of the core material. This effect is additionally reinforced by the afore mentioned dissimilarity in air entrainment, thus leading to too high viscous forces in the model and affecting the flow regime within the breakwater. A lower rate of energy dissipation will result. This subject has been treated by OUMERACI /13/ and JENSEN et al. /8/.

# 7. Concluding Remarks and Perspectives

The present results may be used to estimate reflection, run-up and run-down heights as well as the rate of attenuation of a wave as it propagates into a tetrapod armoured breakwater. However, it should be kept in mind that these results present only a small part of a considerable set of data obtained from systematic tests in large and small-scale models which are now being analysed.

Evaluating in a more systematic and fundamental manner the different energy components in equ. (1) and (2) in order to better understand the complex processes of wave energy dissipation on and in rubble mound breakwaters will be the topic of a forthcoming paper. In addition, an attempt will be made to improve the theory presented in chapter 2. However, in view of the variety and complexity of the interrelated processes involved, like wave breaking and air entrainment, virtual mass effects, non-linearity and unsteadiness of the flow together with the uncertainties in the hydraulic properties of the different breakwater layers, it seems obvious that reliable analytical solutions cannot be developed in a straightforward manner. Therefore, the research strategy adopted at the University of Hannover consists in the development of a reliable integrated numerical code which will be calibrated by the data from the large-scale tests and then used as a research tool, the ultimate objective being the development of analytical solutions.

#### 8. Aknowledgements

This investigation is part of an extensive basic research programme in coastal engineering (SONDERFOR-SCHUNGSBEREICH 205) which is supported by the German Research Council (DFG).

#### 8. References

- 1. BARENDS, F.B.T.: "Geotechnical aspects of rubble mound breakwaters". ICE, Proc. Conf. Breakwater'85, London 1986.
- BIESEL, F.: "Equations de l'écoulement non lent en milieu perméable". - La Houille Blanche No 2, 1950.
- 3. BÜRGER, W.; OUMERACI, H.; PARTENSCKY, H.W.: "Geo-hydraulic investigations on rubble mound breakwaters". ASCE, 21st ICCE, Torremolinos/Spain.
- 4. FÜHRBÖTER, A.: "Über die Bedeutung des Lufteinschlages für die Energieumwandlung in Brandungszonen". Mitteilungen d. Franzius-Instituts, Univ. Hannover, H.36, 1971.
- 5. HALL, K.R.: "A study of the stability of rubble mound breakwaters". - Ph.D. Thesis, Univ. New South Wales/ Australia, 1987.
- 6. HANNOURA, A.A.: "Numerical and experimental modelling of unsteady flow in rockfill embankments". - Ph.D. Thesis, Univ. Windsor, Ontario/Canada, 1978.
- 7. HÖLSHER, P.; DE GROT, M.B.; VAN DE MEER, J.W.: "Simulation of internal water movement in breakwaters". IAHR, SOWAS-Symposium, Delft 1988.
- 8. JENSEN, O.J.; KLINTING, P.: "Evaluation of scale effects in hydraulic models by analysis of laminar and turbulent flow". Coastal Eng. Elsevier, Vol. 7, 1983.
- 9. LEAN, G.H.: "A simplified theory of permeable wave absorbers". IAHR, J. Hydr. Res., 5 (1967) No 1.
- 10.LE MEHAUTE, B.: "Perméabilité des digues en enrochements aux ondes de gravité periodiques". La Houille Blanche No 6, 1957 & No 2, 3, 1958.
- 11.LE MEHAUTE, B.: "Progressive wave absorber". IAHR, J. Hydr. Res. 10 (1972) No 2.
- 12.MICHE; R.: "Recherches théoriques sur les écoulements de filtration non permanents". 5º Journeés de l'Hydraulique, 1960.
- 13.0UMERACI, H.: "Scale effects in coastal hydraulic models". IAHR Symp. on scale effects in modelling hydr. structures, Esslingen, 1984.
- 14. SEELIG; W.N.: "Wave reflection from coastal structures". ASCE, Proc. Conf. Coastal Structures, 1983.
- 15.SIMM, J.D.; HEDGES, T.S.: "Pore pressure response and stability of rubble mound breakwaters". ICE, Breakwater '88, London 1988.